1521-0111/12/8201-125–133
MOLECULAR PHARMACOLOGY
U.S. Government work not protected by U.S. copyright
Mol Pharmacol 82:125–133, 2012

Vol. 82, No. 1
78758/3778394

Balancing Antiviral Potency and Host Toxicity: Identifying a Nucleotide Inhibitor with an Optimal Kinetic Phenotype for HIV-1 Reverse Transcriptase

Christal D. Sohl, Rajesh Kasiviswanathan, Jiae Kim, Ugo Pradere, Raymond F. Schinazi, William C. Copeland, Hiroaki Mitsuya, Masanori Baba, and Karen S. Anderson

Department of Pharmacology, School of Medicine, Yale University, New Haven, Connecticut (C.D.S., J.K., K.S.A.); Laboratory of Molecular Genetics, National Institute of Environmental Health Sciences, National Institutes of Health, Research Triangle Park, North Carolina (R.K., W.C.C.); Center for AIDS Research, Department of Pediatrics, School of Medicine, Emory University, and Department of Veterans Affairs, Atlanta, Georgia (U.P., R.F.S.); Departments of Infectious Diseases and Hematology, Kumamoto University Graduate School of Medical Sciences, Kumamoto, Japan (H.M.); Experimental Retrovirology Section, HIV and AIDS Malignancy Branch, National Cancer Institute, National Institutes of Health, Bethesda, Maryland (H.M.); and Division of Antiviral Chemotherapy, Center for Chronic Viral Diseases, Graduate School of Medical and Dental Sciences, Kagoshima University, Kagoshima, Japan (M.B.)

Received March 14, 2012; accepted April 9, 2012

ABSTRACT

Two novel thymidine analogs, 3′-fluoro-3′-deoxythymidine (FLT) and 2′,3′-didehydro-3′-deoxy-4′-ethynylthymidine (Ed4T), have been investigated as nucleoside reverse transcriptase inhibitors (NRTIs) for treatment of HIV infection. Ed4T seems very promising in phase II clinical trials, whereas toxicity halted FLT development during this phase. To understand these different molecular mechanisms of toxicity, pre–steady-state kinetic studies were used to examine the interactions of FLT and Ed4T with wild-type (WT) human mitochondrial DNA polymerase γ (pol γ), which is often associated with NRTI toxicity, as well as the viral target protein, WT HIV-1 reverse transcriptase (RT). We report that Ed4T-triphosphate (TP) is the first analog to be preferred over native nucleotides by RT but to experience negligible incorporation by WT pol γ, with an ideal balance between high antiretroviral efficacy and minimal host toxicity. WT pol γ could discriminate Ed4T-TP from dTTP 12,000-fold better than RT, with only an 8.3-fold difference in discrimination being seen for FLT-TP. A structurally related NRTI, 2′,3′-didehydro-2′,3′-dideoxythymidine, is the only other analog favored by RT over native nucleotides, but it exhibits only a 13-fold difference (compared with 12,000-fold for Ed4T) in discrimination between the two enzymes. We propose that the 4′-ethynyl group of Ed4T serves as an enzyme selectivity moiety, critical for discernment between RT and WT pol γ. We also show that the pol γ mutation R964C, which predisposes patients to mitochondrial toxicity when receiving 2′,3′-didehydro-2′,3′-dideoxythymidine to treat HIV, produced some loss of discrimination for FLT-TP and Ed4T-TP. These molecular mechanisms of analog incorporation, which are critical for understanding pol γ-related toxicity, shed light on the unique toxicity profiles observed during clinical trials.

Introduction

Since the development of AZT in 1985 (Mitsuya et al., 1985), NRTIs have been vital in the treatment of HIV infection. NRTIs inhibit RT by serving as nucleoside mimics; after phosphorylation by cellular kinases, the inhibitors are incorporated into DNA during reverse transcription. Currently available NRTIs lack a 3′-hydroxyl group, and incorporation causes immediate termination of polymerization. Despite the success of NRTIs, limitations include acquired resistance to

This work was supported by the National Institutes of Health Institute of General Medical Sciences [Grants GM049551, GM099289]; the National Institutes of Health Center for Applied Research [Grant 2P30-AI-050409]; the National Institutes of Health National Institute of Environmental Health Sciences Intramural Research program [Grant ES065080]; and the Atlanta Department of Veteran Affairs.

Article, publication date, and citation information can be found at http://molpharm.aspetjournals.org.

http://dx.doi.org/10.1124/mol.112.078758.

ABBREVIATIONS: AZT, zidovudine; NRTI, nucleoside reverse transcriptase inhibitor; FLT, 3′-fluoro-3′-deoxythymidine; Ed4T, 2′,3′-didehydro-3′-deoxy-4′-ethynylthymidine; EFdA, 4′-ethynyl-2-fluoro-2′-deoxyadenosine; WT, wild-type; RT, reverse transcriptase; pol γ, DNA polymerase γ; exo$^+$ pol γ, exonuclease-competent DNA polymerase γ; dT, thymidine; dA, adenine; TP, triphosphate; MP, monophosphate; FDA, U.S. Food and Drug Administration; d4T, 2′,3′-didehydro-2′,3′-dideoxythymidine; k_{exo}, excision rate; k_{pol}, nucleotide incorporation rate; ddA, 2′,3′-dideoxyadenosine; ddC, 2′,3′-dideoxycytidine.

RT and host toxicity, which can manifest as neuropathy, lactic acidosis, and hepatotoxicity (Apostolova et al., 2011).

Although some toxicity can be attributed to mechanisms such as inhibition of phosphorylation (Apostolova et al., 2011), the primary cause of NRTI toxicity is inhibition of human mitochondrial DNA polymerase γ (pol γ) (Kohler and Lewis, 2007; Koczor and Lewis, 2010). Pol γ, which replicates the human mitochondrial genome, is a heterotrimer containing a catalytic monomer, with polymerization and exonuclease domains, and an accessory homodimer, which improves incorporation efficiency and processivity (Johnson et al., 2000; Lee et al., 2009). Pol γ is a member of the A family of DNA polymerases, which are most similar to RT because of fold commonalities and conserved active site residues (Bienstock and Copeland, 2004). Therefore, pol γ is more prone to insert NRTIs during replication, and side effects are often indicators of mitochondrial toxicity (Brinkman et al., 1999).

The dT-analog NRTIs AZT and d4T (stavudine) have been approved by the FDA for treatment of HIV infection but are plagued by toxicity (Lee et al., 2003), which highlights the need for safer NRTIs. Two dT analogs [i.e., FLT and Ed4T (festinavir)] have been under investigation (Fig. 1). In vitro work showed that FLT inhibited viral replication more effectively than did AZT (Kong et al., 1992), with slow evolution of FLT-resistant mutations in RT (Kim et al., 2001). However, FLT-treated rats experienced mitochondrial DNA depletion (Venhoff et al., 2009). Patient toxicity, including two deaths that resulted from hepatic failure, halted clinical trials in phase II (Flexner et al., 1994). Interest in FLT was renewed somewhat with reports that FLT is effective at lower, less toxic doses (De Clercq, 2010). Phase II clinical trials with Ed4T have proven more promising despite the compound's structural similarity to d4T (which lacks the 4′-ethynyl group), a relatively toxic NRTI that inhibits pol γ (Johnson et al., 2001; Bailey et al., 2009). In vitro studies showed that Ed4T is 5 times more potent and significantly less toxic than d4T (Dutschman et al., 2004; Paintsil et al., 2007), and development of RT resistance is slow (Yang et al., 2009).

Despite documented mitochondrial toxicity for FLT, and the potential for mitochondrial toxicity for Ed4T because of structural similarity to d4T, studies directly probing their interactions with pol γ in relation to RT are limited. Often NRTI potency comes at the expense of toxicity resulting from increased WT pol γ inhibition; therefore, both limited analog incorporation by WT pol γ and efficient incorporation by RT are vital. The ideal balance of potency and toxicity involves more efficient analog incorporation compared with native nucleotides by RT and negligible analog incorporation by WT pol γ. However, this has not yet been achieved.

Previous steady-state studies showed that FLT-TP and Ed4T-TP interact with RT and WT pol γ. Unfortunately, steady-state experiments provide information only on the rate-limiting step of catalysis. For these two polymerases, the rate of polymerization is masked by the slow product-release step. Complete characterization of the analog kinetic profiles was needed, including the analog affinity and incorporation rates for both enzymes and the rates of analog removal by pol γ. Pre–steady-state kinetic data were required to generate these molecular mechanisms of toxicity, which correspond well to the degree of mitochondrial toxicity observed among patients (Johnson et al., 2001). We also examined the R964C pol γ mutant, because patients with this mutation, which is located in the polymerase domain of the pol γ catalytic subunit, exhibit higher rates of mitochondrial toxicity when using d4T (Yamanaka et al., 2007).

We found that WT pol γ was 1400-fold better at distinguishing Ed4T-TP from dTTP than distinguishing FLT-TP from dTTP, and this specificity was moderately impaired in R964C pol γ. Conversely, RT preferred Ed4T-TP to FLT-TP and dTTP. It is noteworthy that Ed4T-TP is the first analog to show this exemplary balance of preferred incorporation by RT and negligible incorporation by WT pol γ. We propose that the didehydro ring of Ed4T (and d4T) is important for achieving impaired discrimination in RT, whereas the 4′-ethynyl group serves as an enzyme selectivity moiety that supports the high level of discrimination by WT pol γ. The unique kinetic mechanisms of interaction for FLT and Ed4T help explain the high levels of toxicity observed for FLT and predict lower levels of toxicity for Ed4T.

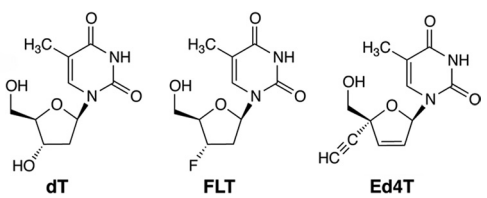

Fig. 1. Structures of dT and its analogs.

Materials and Methods

Reagents. dTTP was purchased from GE Healthcare (Chalfont St. Giles, Buckinghamshire, UK). Triphosphate versions of FLT and Ed4T were prepared as described previously (Ray et al., 2002c). The DNA oligonucleotides D22 (5′-GCCTCGCAGCCGTCCAACCAAC-3′) and D45 (3′-CGGAGCGTCGGCAGGTTGGTTGAGTTGGAGCTAGGTTACGGCAGG-5′) were purchased from Integrated DNA Technologies, Inc. (Coralville, IA) and were purified on 20% polyacrylamide denaturing gels. T4 polynucleotide kinase (New England Biolabs, Ipswich, MA) was used to label the D22 oligonucleotide at the 5′ terminus with [γ-^{32}P]ATP (PerkinElmer Life and Analytical Sciences, Waltham, MA). This D22 primer was then annealed to the D45 template, as described previously (Ray et al., 2002a), to generate the DNA primer/template substrate.

Enzymes. The recombinant WT accessory subunit of pol γ was expressed and purified as described previously (Johnson et al., 2000). All pol γ catalytic subunits used contained an N-terminal hexahistidine tag. The recombinant, exonuclease-deficient, WT catalytic subunit (i.e., WT pol γ) was expressed and purified as described previously (Graziewicz et al., 2004), with minor modifications in the strategy for chromatography. Specifically, WT pol γ was eluted from a nickel column by using a linear gradient of 20 to 400 mM imidazole. The recombinant exonuclease-competent pol γ catalytic subunit (exo$^+$ pol γ) was expressed and purified as described previously (Longley et al., 1998; Lim et al., 2003; Kasiviswanathan et al., 2010). Site-directed mutagenesis was used to generate the R964C pol γ construct, and the recombinant protein was expressed and purified as detailed elsewhere (Kasiviswanathan et al., 2010).

The recombinant RT (p66/p51 heterodimer) clone was kindly provided by Drs. Stephen Hughes and Andrea Ferris (Frederick Cancer Research and Development Center, Frederick, MD). The C-terminal hexa-histidine-tagged RT was purified as described previously (Kerr and Anderson, 1997; Kim et al., 2012). The purity of all proteins, as judged through SDS-polyacrylamide gel electrophoresis with Coomassie staining, was >90%.

Single-Nucleotide Incorporation Assays. Single-nucleotide incorporation experiments were performed by using a KinTek RQF-3

rapid chemical quench apparatus (KinTek Corp., Austin, TX) operated at 37°C. To determine the active-site concentration of each of the enzymes used, dTTP incorporation into the D22/D45 primer/template substrate was examined under burst conditions, as described previously (Murakami et al., 2003). Single-turnover conditions were used to examine the rates of dTTP, FLT-TP, and Ed4T-TP incorporation. For incorporation by WT pol γ and R964C pol γ, 100 nM pol γ catalytic subunit (active-site concentration) was preincubated with an excess of pol γ accessory subunit (4-fold higher concentration than the total, non–active-site, concentration of the catalytic subunit). Holoenzyme (heterotrimer) at 100 nM and 25 nM DNA primer/template substrate in pol γ reaction buffer (50 mM Tris, pH 7.8 at 37°C, 100 mM NaCl) were rapidly mixed with 2.5 mM $MgCl_2$ and varying concentrations of dTTP or analog. Single-nucleotide incorporation experiments with RT were performed in the same manner as the pol γ experiments except that 100 nM RT was used instead of pol γ holoenzyme. Reported concentrations are final (after mixing). After pre–steady-state time periods, the reactions were quenched with 0.3 M EDTA, pH 8.0, and the products were separated on 20% polyacrylamide denaturing gels (0.4 mm thick; 8 M urea). After quantification through filmless autoradiographic analysis with a Bio-Rad Molecular Imager FX (Bio-Rad, Hercules, CA), Kaleidagraph software (Synergy Software, Reading, PA) was used to fit plots of product concentrations versus time to a single exponential equation: product concentration = $A[1 - \exp(-k_{obs}t)]$, where A is the amplitude, k_{obs} is the observed first-order rate constant for dTTP or analog incorporation, and t is the reaction time. The k_{obs} values were plotted against nucleotide concentrations to generate the maximal nucleotide incorporation rate (k_{pol}) and K_d (i.e., the dissociation constant for the nucleotide at the enzyme-primer/template substrate complex) through fitting to a hyperbolic equation: $k_{obs} = (k_{pol} \times \text{dNTP concentration})/(K_d + \text{dNTP concentration})$, with Kaleidagraph software.

Excision Reactions. To incorporate FLT-TP into the 5′-radiolabeled D22/D45 primer/template substrate, 8.0 μM FLT-TP, 5.0 μM DNA primer/template substrate, 1 μM WT pol γ holoenzyme, and 10 mM $MgCl_2$ were incubated for 3 h in pol γ reaction buffer at 37°C. For Ed4T-TP incorporation, 30 μM Ed4T-TP, 5.0 μM DNA primer/template substrate, 1.0 μM RT, and 10 mM $MgCl_2$ were incubated for 2 h in RT reaction buffer (50 mM Tris, pH 7.8 at 37°C, 50 mM NaCl) at 37°C. The reactions were optimized such that the analog incorporation reaction achieved completion. The remaining experimental parameters were the same for both FLT-MP and Ed4T-MP. The incubation mixtures were purified on 20% denaturing polyacrylamide sequencing gels (8 M urea) and, by using filmless autoradiographic analysis, the radiolabeled band, corresponding to D22 with the analog incorporated at position 23 (D22-FLT-MP or D22-Ed4T-MP), was removed. The DNA was extracted from the gel through gentle mixing overnight at room temperature, in a solution containing 0.5 M ammonium acetate, 20 mM magnesium acetate, 1 mM EDTA, and 0.1% SDS. After ethanol extraction (with a 75% ethanol solution for 4 h at −80°C) and drying, the D22-analog primer was rephosphorylated and reannealed as described previously, to generate the DNA primer-analog/template substrate (Ray et al., 2002a). An incubation of 150 nM exo^+ pol γ holoenzyme and 112 nM DNA primer-analog/template substrate in pol γ reaction buffer was manually mixed with 5 mM $MgCl_2$ to initiate the excision reaction at 37°C, under single-turnover conditions. All reported concentrations are final (after mixing). Aliquots of the mixture were removed at various time points and quenched with 0.3 M EDTA, pH 8.0. A 20% denaturing polyacrylamide sequencing gel (0.4 mm thick, 8 M urea) was used to separate the products, and filmless autoradiographic analysis was used to quantify the loss of substrate. A plot of percent substrate versus time was fit to a single exponential decay equation to generate the excision rate (k_{exo}). For Ed4T-MP excision, the plot was fit to a Boltzman sigmoidal equation, and the inflection point concentration was used to determine the half-life, which is proportional to k_{exo} under pseudo-first-order kinetics.

Results

FLT-TP and Ed4T-TP Discrimination by WT pol γ. A critical component of the in vitro toxicity profiles for novel NRTIs is the extent of incorporation by WT pol γ. Previous data on the interactions of these inhibitors with WT pol γ were limited to IC_{50} of 2.7 μM (Cheng et al., 1987) and K_i of 50 nM (Wińska et al., 2010) for FLT-TP and IC_{50} of 100 μM for Ed4T-TP [100-fold higher than that for d4T-TP (Yang et al., 2007)]. Steady-state kinetic data reflect only the rate-limiting step of catalysis, which is product release for many polymerases, including WT pol γ. Therefore, rate constants associated with polymerization cannot be determined from such studies. We used pre–steady-state kinetic analyses to determine the k_{pol} and K_d for FLT-TP and Ed4T-TP incorporation, relative to dTTP.

Under single-turnover conditions, WT pol γ holoenzyme and the DNA primer/template substrate were rapidly mixed with $MgCl_2$ and varying concentrations of dTTP, FLT-TP, or Ed4T-TP for varying times. Triphosphate versions of the drugs were used because the cellular kinases required to phosphorylate the NRTI prodrugs were not present in these in vitro studies. After reaction quenching, the products were separated through gel electrophoresis, and filmless autoradiographic analysis allowed quantification of incorporation of the single correct nucleotide to form the D23 product. The amount of product formed was plotted against the reaction time. This was fit to a single exponential equation to generate the observed rate of nucleotide incorporation, k_{obs}, at each concentration (Fig. 2). These k_{obs} values were then plotted against nucleotide incorporation and fit to a hyperbola to generate k_{pol} and K_d values (Fig. 3).

WT pol γ was able to incorporate dTTP with very high efficiency. The k_{pol} for FLT-TP incorporation by WT pol γ was ~260-fold slower than that for dTTP incorporation (Table 1). However, the affinity for FLT-TP was actually 7.5-fold greater than that for dTTP, which means that WT pol γ preferred the nucleoside analog on the basis of K_d alone. Because of this finding, the overall efficiency of FLT-TP incorporation was only 35-fold lower than that of dTTP incorporation, which indicates that FLT-TP may serve as a substrate for WT pol γ in vivo to a modest but significant extent. This kinetic profile of FLT-TP interaction with WT pol γ supports the evidence of mitochondrial toxicity in vitro (de Baar et al., 2007) and in vivo (Venhoff et al., 2009).

Ed4T-TP demonstrated a different kinetic mechanism of interaction with WT pol γ, compared with that seen for FLT-TP. The k_{pol} for Ed4T-TP incorporation was 2100-fold and 7.9-fold slower than those for dTTP and FLT-TP, respectively (Table 1). Ed4T-TP also showed superiority to FLT-TP in its weak affinity for WT pol γ, with 3- and 23-fold increases in K_d, compared with dTTP and FLT-TP, respectively. Overall, impressive 6200-fold and 180-fold decreases in incorporation efficiency were seen for Ed4T-TP relative to dTTP and FLT-TP, respectively. This high level of discrimination against Ed4T-TP indicates that incorporation of this inhibitor in the physiological nucleotide milieu, where individual dNTP concentrations range from low micromolar to submillimolar levels in mammalian (rat) mitochondria (Song et al., 2005; Wheeler and Mathews, 2011), probably is a rare event. This is supported by the findings of low toxicity in vitro (Haraguchi et al., 2003; Dutschman et al., 2004; Tanaka et al., 2005).

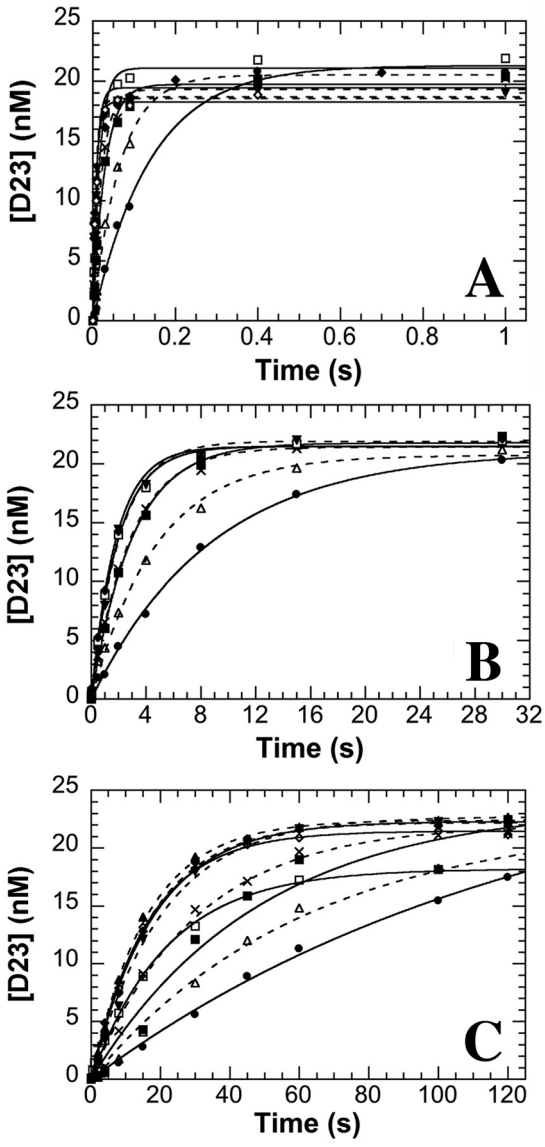

Fig. 2. Observed rates of incorporation by WT pol γ of dTTP or dTTP analogs opposite dA. Each point in the plot represents a single observation, and single exponential equations were used to fit the kinetic traces at varying concentrations of dTTP or dTTP analog. These six to eight experiments all contributed to the k_{pol} and K_d rate constant values. A, incorporation of dTTP. Concentrations of dTTP are denoted as follows: ●, 0.20 μM; △, 0.40 μM; ■, 0.80 μM; ×, 1.5 μM; □, 3.0 μM; ▼, 6.0 μM; ♦, 8 μM; +, 13 μM; ◇, 20 μM. B, incorporation of FLT-TP. Concentrations of FLT-TP are denoted as follows: ●, 0.10 μM; △, 0.25 μM; ■, 0.50 μM; ×, 1.0 μM; □, 2.0 μM; ▼, 5.0 μM; ♦, 8.0 μM. C, incorporation of Ed4T-TP. Concentrations of Ed4T-TP are denoted as follows: ●, 1.5 μM; △, 2.5 μM; ■, 5.0 μM; ×, 8.0 μM; □, 10 μM; ▼, 20 μM; ♦, 30 μM; +, 40 μM; ◇, 50 μM; ▲, 75 μM.

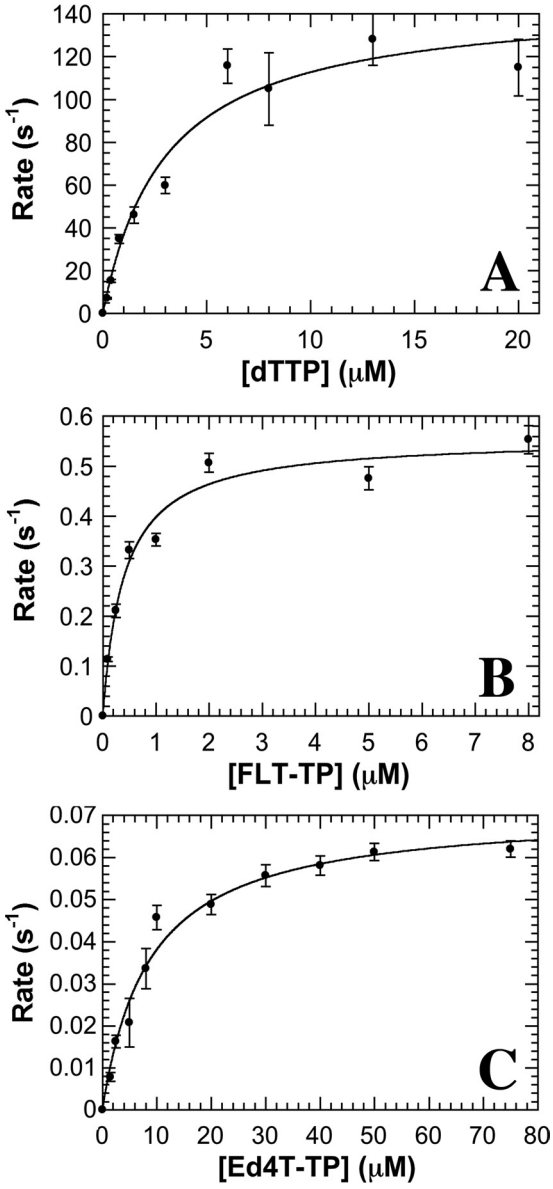

Fig. 3. Nucleotide concentration dependence of the observed rate of WT pol γ incorporation of dTTP analogs opposite dA. Hyperbolic equations were used to fit plots of the observed rate constants (generated from Fig. 2) versus dTTP analog concentrations to obtain k_{pol} and K_d values. Each point represents the observed rate generated from Fig. 2, and the S.E. is the deviance from the hyperbolic fits. Values for k_{pol}, K_d, and efficiency are presented in Table 1. A, incorporation of dTTP. B, incorporation of FLT-TP. C, incorporation of Ed4T-TP.

FLT-TP and Ed4T-TP Discrimination by RT. The characterization of the interactions of these analogs with RT is limited, with previous findings including a K_i value of 5 nM for the inhibition of RT by FLT-TP (Cheng et al., 1987) and pre–steady-state studies showing that RT preferred dTTP 1.9-fold over Ed4T-TP, compared with a 4.5-fold preference for dTTP over d4T (Yang et al., 2008). We undertook pre–steady-state, single-turnover experiments in which RT and the DNA-primer/template substrate were rapidly mixed with $MgCl_2$ and varying concentrations of dTTP, FLT-TP, or Ed4T-TP (Fig. 4).

A 2.2-fold decrease in k_{pol} and a 2-fold increase in K_d were observed for FLT-TP incorporation by RT, relative to dTTP, which resulted in 4.2-fold greater efficiency for dTTP, compared with FLT-TP (Fig. 5 and Table 1). Although there was some preference for the native nucleotide, the incorporation efficiency, which was similar to that for dTTP, indicated that RT would incorporate FLT-TP at significant rates in vivo. The k_{pol} for Ed4T-TP incorporation was identical to that of dTTP. It is noteworthy that the binding affinity was greater, as evidenced by the 2-fold decrease in K_d relative to dTTP, which indicates that RT incorporated Ed4T-TP 2.0-fold more efficiently than dTTP (Fig. 5 and Table 1).

The discrimination by WT pol γ (Table 1) compared favorably with that of RT. RT showed a 8.3-fold loss of discrimi-

TABLE 1
Kinetic parameters for WT pol γ, RT, and R964C pol γ
Efficiency indicates k_{pol}/K_d. Discrimination indicates efficiency$_{dTTP}$/efficiency$_{analog}$.

Enzyme and dTTP Analog	k_{pol}	K_d	Efficiency	Discrimination
	s^{-1}	μM	$\mu M^{-1}\ s^{-1}$	
WT pol γ				
dTTP	147 ± 12	3.0 ± 0.8	49	N.A.
FLT-TP	0.56 ± 0.03	0.40 ± 0.08	1.4	35
Ed4T-TP	0.071 ± 0.003	9 ± 1	0.0079	6200
RT				
dTTP	1.25 ± 0.06	3.0 ± 0.4	0.42	N.A.
FLT-TP	0.58 ± 0.05	6 ± 1	0.1	4.2
Ed4T-TP	1.25 ± 0.05	1.5 ± 0.2	0.83	0.51
R964C pol γ				
dTTP	129 ± 8	3.7 ± 0.7	35	N.A.
FLT-TP	0.51 ± 0.03	0.23 ± 0.06	2.2	16
Ed4T-TP	0.11 ± 0.01	7 ± 2	0.02	1800

N.A., not applicable.

nation for FLT-TP incorporation, relative to WT pol γ, and a striking 12,000-fold decrease in discrimination was seen when Ed4T-TP incorporation by RT was compared with that by WT pol γ. RT is much more likely to incorporate these inhibitors than is WT pol γ. These findings can explain the low toxicity observed to date for Ed4T-TP, although additional clinical testing is needed.

Excision of FLT-MP and Ed4T-MP by exo$^+$ pol γ. An important consideration in the in vitro toxicity profile regarding NRTI incorporation by pol γ is the enzyme's inherent proofreading capability. Nucleoside analog incorporation by pol γ can be essentially negated if excision is efficient. On the basis of nucleoside analog incorporation efficiency, either WT pol γ or RT was used to incorporate a single FLT-TP or a single Ed4T-TP into the DNA primer/template substrate. The D22-FLT-MP/D45 or D22-Ed4T-MP/D45 primer/template was then used as a substrate in the excision reaction. Under single-turnover conditions, exo$^+$ pol γ holoenzyme and the DNA primer-analog/template substrate were manually mixed with $MgCl_2$, and the reaction was quenched after various times. After separation of the products through gel electrophoresis and quantification of the substrate band, the proportion of substrate was plotted versus time (Fig. 6) and the data were fit to a single exponential equation to obtain k_{exo} values, as well as a sigmoidal equation in the case of Ed4T-MP excision (Fig. 6B, inset).

FLT-MP and Ed4T-MP were excised at similar modest rates, although Ed4T-MP excision was slower with the sigmoidal fit (Fig. 6). Half-lives for the exo$^+$ pol γ·D22-analog/D45 complex were 8.8 and 9.6 min for FLT and Ed4T, respectively. These rates of excision were approximately 34-fold slower, on average, than the excision rate for a correctly inserted dT for this primer/template substrate (0.042 s^{-1}) (Feng et al., 2001). However, both analogs were removed more efficiently than ddC and ddA, which have k_{exo} values of 0.0003 s^{-1} (Hanes and Johnson, 2008) and 0.0005 s^{-1} (Johnson et al., 2001), respectively.

FLT-TP and Ed4T-TP Discrimination by R964C pol γ. It was established that d4T-treated patients with the R964C pol γ mutation have higher rates of mitochondrial toxicity (Yamanaka et al., 2007), primarily because of moderate defects in activity and lower levels of nucleoside analog discrimination (Bailey et al., 2009). To determine whether such alterations in pol γ activity were extended to other dTTP analogs, the single-turnover, pre–steady-state experiments performed with WT pol γ were repeated with the R964C pol γ holoenzyme (Fig. 7). Such studies are important to determine whether patients with the R964C pol γ mutation who receive FLT or Ed4T are at higher risk for mitochondrial toxicity.

The incorporation efficiency of dTTP decreased only slightly (1.4-fold) relative to WT pol γ (Table 1), which is consistent with the 1.5-fold loss of efficiency measured previously (Bailey et al., 2009). R964C pol γ was able to incorporate FLT-TP with slightly (1.6-fold) higher efficiency than WT pol γ, and Ed4T-TP was incorporated 2.5-fold more efficiently by R964C pol γ than by WT pol γ (Table 1). When overall discrimination (which takes into account defects in dTTP incorporation) was considered, R964C pol γ showed 2.2-fold and 3.4-fold decreases in discrimination for FLT-TP and Ed4T-TP, respectively, relative to WT pol γ (Table 1).

Discussion

The interactions of FLT-TP and Ed4T-TP with WT pol γ and RT were unique, which clarified the reported differences in toxicity. The incorporation of FLT-TP by WT pol γ was 35-fold slower than that of dTTP, similar to findings for the more toxic NRTIs on the market, compared with the 1000- to nearly 1,000,000-fold slower incorporation for other low-toxicity inhibitors (Table 2). This indicates that some toxicity results from FLT-TP incorporation. On the basis of affinity alone, FLT-TP was preferred over dTTP by WT pol γ. Studies examining the potential for toxicity have focused on pol γ with the analog as a substrate, but we propose that this low K_d indicates that the mitochondrial toxicity observed for FLT may result from direct inhibition. It is likely to be more complex than simple competition, because it was shown that FLT-TP is a noncompetitive inhibitor of pol γ (Wińska et al., 2010). It was proposed that mitochondrial toxicity results in part from competitive inhibition of host thymidine kinase 2 by FLT (Wang et al., 2011), and it is likely that many factors contribute to FLT toxicity.

Ideally, discrimination against dNTP analogs by WT pol γ would be high, whereas discrimination by RT would be low. This would indicate that WT pol γ could readily distinguish among NRTIs and native nucleotides, whereas RT could not. There is only a slight preference for dTTP over FLT-TP with RT, which compares favorably to data for many FDA-approved NRTIs and inhibitors under development (Table 2).

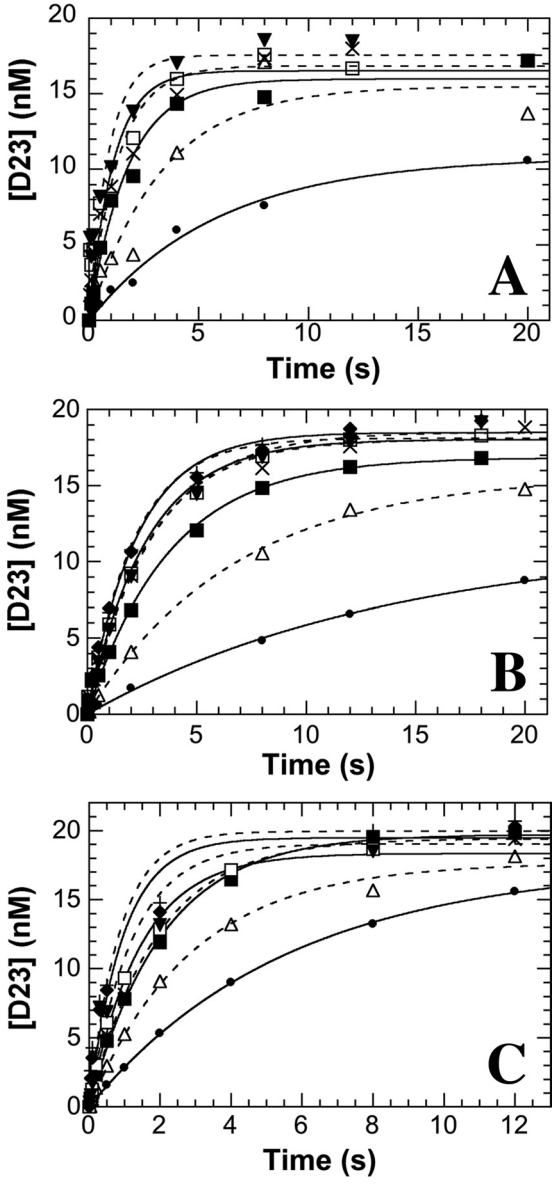

Fig. 4. Observed rates of incorporation by RT of dTTP or dTTP analogs opposite dA. Each point in the plot represents a single observation, and single exponential equations were used to fit the kinetic traces at varying concentrations of dTTP or dTTP analog. These six to eight experiments all contributed to the k_{pol} and K_d rate constant values. A, incorporation of dTTP. Concentrations of dTTP are denoted as follows: ●, 0.50 μM; △, 1.0 μM; ■, 2.0 μM; ×, 4.0 μM; □, 10 μM; ▼, 20 μM. B, incorporation of FLT-TP. Concentrations of FLT-TP are denoted as follows: ●, 0.50 μM; △, 2.0 μM; ■, 5.0 μM; ×, 8.0 μM; □, 10 μM; ▼, 12 μM; ♦, 16 μM; +, 20 μM. C, incorporation of Ed4T-TP. Concentrations of Ed4T-TP are denoted as follows: ●, 0.20 μM; △, 0.60 μM; ■, 1.0 μM; ×, 1.4 μM; □, 1.8 μM; ▼, 2.0 μM; ♦, 8.0 μM; +, 20 μM.

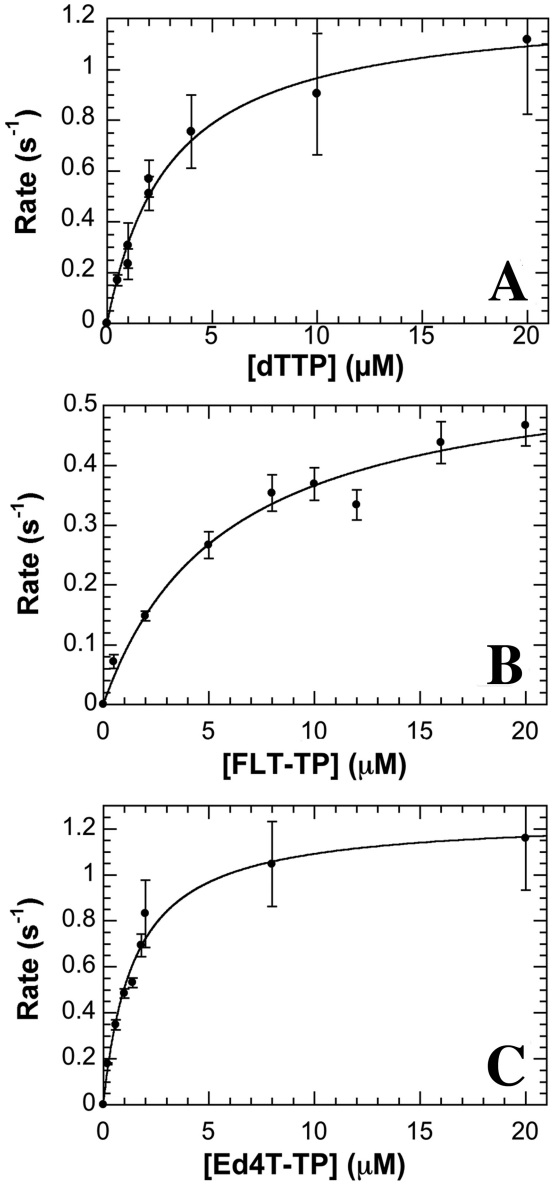

Fig. 5. Nucleotide concentration dependence of the observed rate of RT incorporation of dTTP analogs opposite dA. Hyperbolic equations were used to fit plots of the observed rate constants (generated from Fig. 4) versus dTTP analog concentrations to obtain k_{pol} and K_d values. Each point represents the observed rate generated from Fig. 4, and the S.E. is the deviance from the hyperbolic fits. Values for k_{pol}, K_d, and efficiency are presented in Table 1. A, incorporation of dTTP. B, incorporation of FLT-TP. C, incorporation of Ed4T-TP.

This supports the finding that lower doses of FLT are effective and less toxic (see above). WT pol γ very successfully discriminated against Ed4T-TP, showing 6200- and 180-fold greater discrimination, relative to values for dTTP and FLT-TP, respectively. This strikingly high level of selectivity is better than values for many currently available NRTIs (Table 2). Furthermore, in contrast to the very high level of selectivity shown by WT pol γ, RT showed very low discrimination between Ed4T-TP and dTTP. In fact, Ed4T-TP was the preferred substrate. This preference seems to be sequence-dependent, because a study using a different DNA primer/template substrate found a modest preference for dTTP over Ed4T-TP (Yang et al., 2008).

We showed that RT was poor at discriminating Ed4T and d4T from dTTP, with discrimination values of 0.51 and 0.56, respectively (Vaccaro et al., 2000) (Table 2); the preference for these two analogs over dTTP is unique among all of the NRTIs assayed to date (Table 2). The didehydro ring found in d4T and Ed4T may facilitate incorporation by RT and limit the discrimination of these analogs from the native nucleotides. Whereas d4T-TP was preferred over dTTP by RT, the corresponding selectivity by WT pol γ was 840-fold lower than for Ed4T-TP (Table 2) (Vaccaro et al., 2000; Johnson et al., 2001). Although RT preferred both analogs, there was a 13-fold difference in discrimination between RT and WT pol

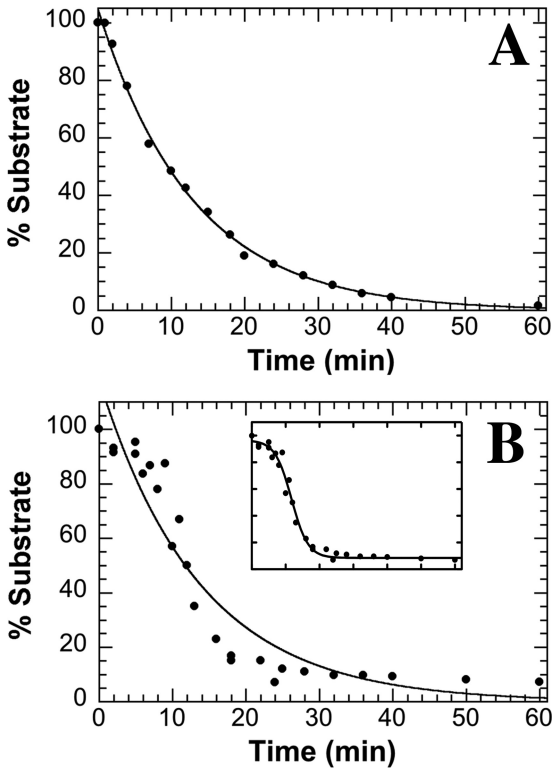

Fig. 6. Rates of dTTP analog excision by exo$^+$ pol γ. Single exponential decay equations were used to determine k_{exo} values. A, excision of FLT-MP (k_{exo} = 0.00130 ± 0.00005 s^{-1}). B, excision of Ed4T-MP (k_{exo} = 0.0012 ± 0.0002 s^{-1}). Inset, sigmoidal fit of the data (k_{exo} = 0.00018 s^{-1}).

γ for d4T-TP, compared with a 12,000-fold difference in discrimination for Ed4T-TP. To our knowledge, Ed4T is the first NRTI to serve both as a preferred substrate for RT and as a nearly negligible substrate for WT pol γ.

Because the only difference between d4T and Ed4T is the presence of the 4′-ethynyl group, this functionality may serve as an enzyme selectivity moiety, in that discrimination by WT pol γ (but importantly not RT) improves 840-fold when the ethynyl group is present (Table 2). It is likely that a similar trend would be seen with 4′-ethynyl-2-fluoro-2′-deoxyadenosine (EFdA)-TP; we found a 4300-fold preference for dATP over EFdA-TP with WT pol γ (Sohl et al., 2012), and steady-state studies with RT yielded a discrimination value of 0.5 (i.e., EFdA-TP is preferred over dATP) (Michailidis et al., 2009). NMR spectroscopy studies probing the interaction of RT and EFdA indicated that the 4′-ethynyl group locks the sugar into a conformation favorable for incorporation by RT but not WT pol γ, which contributes to the preference of RT for the analog (Kirby et al., 2011). The 4′-ethynyl group may serve as an enzyme selectivity moiety in Ed4T, although structural studies would be required to assess this.

A more subtle characteristic of the poor discrimination shown by RT for FLT-TP and Ed4T-TP concerns the development of resistance. The rate of generation of NRTI resistance mutations in RT after d4T treatment occurs notably more slowly than with other NRTIs (Lin et al., 1994). It was proposed that this is attributable, at least in part, to poor discrimination by RT (Vaccaro et al., 2000; Ray et al., 2002b). Our findings of low levels of RT discrimination can provide an explanation for the observed slow RT mutation rates for FLT and Ed4T (Kim et al., 2001; Nitanda et al., 2005; Yang et al., 2009). We also note that important future work includes testing the efficiency of incorporation of FLT-TP and Ed4T-TP with RT containing NRTI-resistant mutations to predict effectiveness among NRTI-experienced patients.

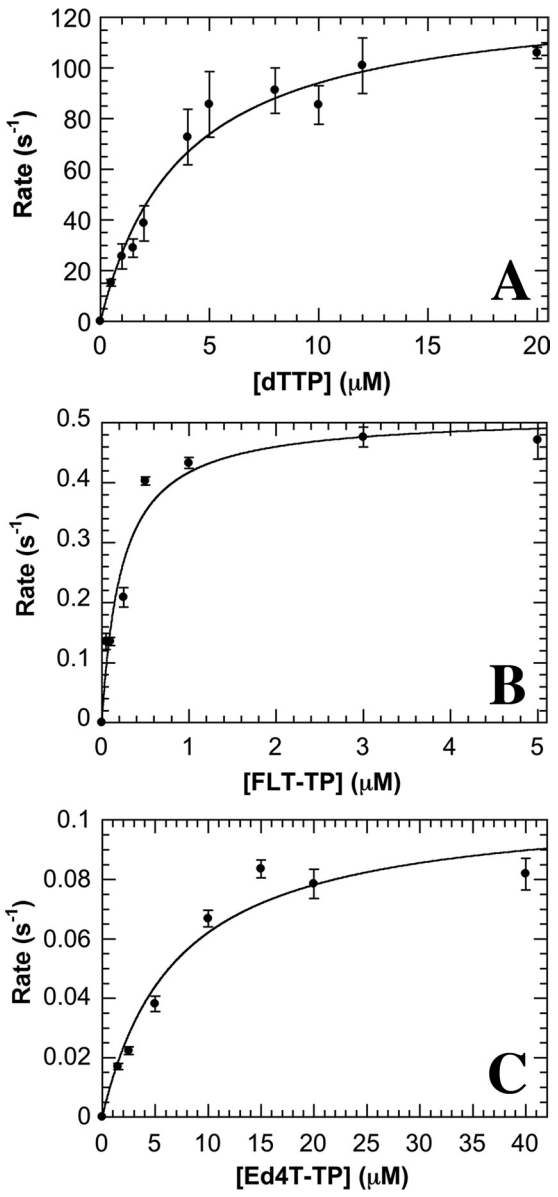

Fig. 7. Nucleotide concentration dependence of the observed rate of R964C pol γ incorporation of dTTP analogs opposite dA. Hyperbolic equations were used to fit plots of the observed rate constants versus dTTP analog concentrations to obtain k_{pol} and K_d values. Each point represents the observed rate generated by fitting a time course with 10 different points to a single exponential expression, and the S.E. is the deviance from the hyperbolic fits. Values for k_{pol}, K_d, and efficiency are presented in Table 1. A, incorporation of dTTP. B, incorporation of FLT-TP. C, incorporation of Ed4T-TP.

Both FLT-MP and Ed4T-MP were excised somewhat efficiently from the primer/template substrate by exo$^+$ pol γ (Fig. 6). Although a single exponential equation fit well the data measured for FLT-MP excision (Fig. 6A), a very slight sigmoidal characteristic of Ed4T-MP excision (Fig. 6B) resulted in a minor deviation from a similar fit. This initial slow phase caused a slower rate of excision when a sigmoidal fit was used (Fig. 6B, inset). It is possible that excision of Ed4T-MP requires a more complicated reaction scheme (i.e.,

TABLE 2

Comparison of efficiency of WT pol γ and RT incorporation of nucleoside analogs, FDA-approved NRTIs, and NRTIs under development

Discrimination (efficiency$_{dNTP}$/efficiency$_{analog}$) is shown, rather than incorporation efficiency, to minimize the rate constant variations associated with different primer/template substrates.

dNTP Analog	Discrimination		Reference
	WT pol γ	RT	
ddC-TP	2.9	10	Feng and Anderson, 1999; Feng et al., 2001; Ray et al., 2003
ddA-TP	4.0	5	Johnson et al., 2001
d4T-TP	7.4	0.56	Vaccaro et al., 2000; Johnson et al., 2001
KP1212-TP	26	14	Murakami et al., 2005
FLT-TP	35	4.2	Current study
(−)-3TC-TP	2900	40	Feng and Anderson, 1999; Feng et al., 2001; Ray et al., 2003
EFdA-TP	4300	N.D.[a]	Sohl et al., 2012
Ed4T-TP	6200	0.51	Current study
PMPApp	11,400	6.1	Johnson et al., 2001
AZT-TP	37,000	2.7	Vaccaro and Anderson, 1998; Johnson et al., 2001
(−)-FTC-TP	290,000	16	Feng et al., 2004
CBV-TP	900,000	34	Johnson et al., 2001

N.D., no data; KP1212, 5-aza-5,6-dihydro-2'-deoxycytidine; 3TC, lamivudine; PMPApp, tenofovir diphosphate; FTC, emtricitabine; CBV, carbovir.
[a] Steady-state studies indicated an efficiency of 0.5 (Michailidis et al., 2009).

more steps) than does excision of FLT-MP, including conformational changes or changes related to partitioning between the two active sites. Without structural or spectral evidence to support this, our focus is on the single exponential fit, although experimentally testing alternate reaction schemes is an interest for future study. The rate of dissociation of a DNA template is ~0.02 s^{-1} (Johnson and Johnson, 2001), and it is likely that DNA dissociation upon dTTP analog incorporation occurs more often than excision.

The moderate excision rates for FLT-MP and Ed4T-MP are within the range of values for most FDA-approved NRTIs (Johnson et al., 2001) and are faster than the rates of removal of ddC (0.0003 s^{-1}) (Hanes and Johnson, 2008) and ddA (0.0005 s^{-1}) (Johnson et al., 2001). Our finding of the faster (relative to ddC and ddA) Ed4T excision rate supports work examining the link between the dissociation constant of the incoming nucleotide analog and the kinetic partitioning of the DNA in the pol γ polymerase and exonuclease active sites (Hanes and Johnson, 2008). Specifically, the low affinity of WT pol γ for Ed4T may facilitate transfer of the DNA primer/template from the polymerase active site to the exonuclease active site during excision. Affinity constants for ddC-TP (Feng et al., 2001) and ddA-TP (Johnson et al., 2001), which are excised much more slowly by exo^+ pol γ, indicate that they bind much more tightly than Ed4T. Likewise, the K_d for FLT-TP is 1 order of magnitude greater than those of ddC-TP and ddA-TP (Johnson et al., 2001), which suggests more favorable excision active site partitioning for FLT removal, compared with ddC and ddA, to help achieve the faster rate of FLT excision.

As seen with d4T treatment (Yamanaka et al., 2007), we predict that patients with the R964C pol γ mutation may show higher rates of mitochondrial toxicity. As noted for d4T (Bailey et al., 2009), alterations in incorporation kinetics were modest but significant; R964C pol γ incorporated dTTP 1.4-fold less efficiently than WT pol γ, and FLT-TP and Ed4T-TP were incorporated 1.6- and 2.5-fold more efficiently, respectively [compared with 2.1-fold more efficiently for d4T-TP (Bailey et al., 2009)] (Table 1). This resulted in overall 2.2- and 3.4-fold losses of discrimination for dTTP over FLT-TP and Ed4T-TP, respectively (Table 1), similar to the 3.2-fold loss of discrimination for dTTP over d4T-TP determined previously (Bailey et al., 2009). Using these dTTP analogs for patients with the R964C pol γ mutation may lead to higher rates of mitochondrial toxicity because of the similar kinetic profiles, compared with d4T (Yamanaka et al., 2007), although it is possible that other toxicity mechanisms also may contribute. This mutation should be taken into consideration when FLT and Ed4T are tested in clinical settings.

In summary, we found that two relatively new RT inhibitors for treatment of HIV infection, FLT-TP and Ed4T-TP, were incorporated by WT pol γ nearly 1 and >3 orders of magnitude more slowly, respectively, than dTTP. RT readily incorporated both inhibitors, however, and actually preferred Ed4T-TP over native nucleotides. Ed4T is the first NRTI shown to be preferred by RT and yet have negligible incorporation by WT pol γ. We propose that the ethynyl group in Ed4T serves as an enzyme selectivity moiety to generate the different discrimination abilities of RT and WT pol γ, which is an important finding for future NRTI design. These unique kinetic interaction profiles for FLT-TP and Ed4T-TP provide a mechanism to explain the different susceptibilities to toxicity. Such studies are critical for understanding pol γ-mediated mechanisms of toxicity for NRTIs in preclinical and clinical trials.

Acknowledgments

We thank Dr. Ligong Wang for expression and purification of the WT pol γ accessory subunit.

Authorship Contributions

Participated in research design: Sohl and Anderson.
Conducted experiments: Sohl and Kim.
Contributed new reagents or analytic tools: Kasiviswanathan, Pradere, Schinazi, Copeland, Mitsuya, and Baba.
Performed data analysis: Sohl and Kim.
Wrote or contributed to the writing of the manuscript: Sohl and Anderson.

References

Apostolova N, Blas-García A, and Esplugues JV (2011) Mitochondrial interference by anti-HIV drugs: mechanisms beyond Pol-γ inhibition. *Trends Pharmacol Sci* **32:** 715–725.

Bailey CM, Kasiviswanathan R, Copeland WC, and Anderson KS (2009) R964C mutation of DNA polymerase gamma imparts increased stavudine toxicity by decreasing nucleoside analog discrimination and impairing polymerase activity. *Antimicrob Agents Chemother* **53:**2610–2612.

Bienstock RJ and Copeland WC (2004) Molecular insights into NRTI inhibition and mitochondrial toxicity revealed from a structural model of the human mitochondrial DNA polymerase. *Mitochondrion* **4:**203–213.

Brinkman K, Smeitink JA, Romijn JA, and Reiss P (1999) Mitochondrial toxicity induced by nucleoside-analogue reverse-transcriptase inhibitors is a key factor in

the pathogenesis of antiretroviral-therapy-related lipodystrophy. *Lancet* **354:** 1112–1115.
Cheng YC, Dutschman GE, Bastow KF, Sarngadharan MG, and Ting RY (1987) Human immunodeficiency virus reverse transcriptase. General properties and its interactions with nucleoside triphosphate analogs. *J Biol Chem* **262:**2187–2189.
de Baar MP, de Rooij ER, Smolders KG, van Schijndel HB, Timmermans EC, and Bethell R (2007) Effects of apricitabine and other nucleoside reverse transcriptase inhibitors on replication of mitochondrial DNA in HepG2 cells. *Antiviral Res* **76:**68–74.
De Clercq E (2010) Antiretroviral drugs. *Curr Opin Pharmacol* **10:**507–515.
Dutschman GE, Grill SP, Gullen EA, Haraguchi K, Takeda S, Tanaka H, Baba M, and Cheng YC (2004) Novel 4′-substituted stavudine analog with improved anti-human immunodeficiency virus activity and decreased cytotoxicity. *Antimicrob Agents Chemother* **48:**1640–1646.
Feng JY and Anderson KS (1999) Mechanistic studies comparing the incorporation of (+) and (−) isomers of 3TCTP by HIV-1 reverse transcriptase. *Biochemistry* **38:**55–63.
Feng JY, Johnson AA, Johnson KA, and Anderson KS (2001) Insights into the molecular mechanism of mitochondrial toxicity by AIDS drugs. *J Biol Chem* **276:**23832–23837.
Feng JY, Murakami E, Zorca SM, Johnson AA, Johnson KA, Schinazi RF, Furman PA, and Anderson KS (2004) Relationship between antiviral activity and host toxicity: comparison of the incorporation efficiencies of 2′,3′-dideoxy-5-fluoro-3′-thiacytidine-triphosphate analogs by human immunodeficiency virus type 1 reverse transcriptase and human mitochondrial DNA polymerase. *Antimicrob Agents Chemother* **48:**1300–1306.
Flexner C, van der Horst C, Jacobson MA, Powderly W, Duncanson F, Ganes D, Barditch-Crovo PA, Petty BG, Baron PA, and Armstrong D (1994) Relationship between plasma concentrations of 3′-deoxy-3′-fluorothymidine (alovudine) and antiretroviral activity in two concentration-controlled trials. *J Infect Dis* **170:** 1394–1403.
Graziewicz MA, Longley MJ, Bienstock RJ, Zeviani M, and Copeland WC (2004) Structure-function defects of human mitochondrial DNA polymerase in autosomal dominant progressive external ophthalmoplegia. *Nat Struct Mol Biol* **11:**770–776.
Hanes JW and Johnson KA (2008) Exonuclease removal of dideoxycytidine (zalcitabine) by the human mitochondrial DNA polymerase. *Antimicrob Agents Chemother* **52:**253–258.
Haraguchi K, Takeda S, Tanaka H, Nitanda T, Baba M, Dutschman GE, and Cheng YC (2003) Synthesis of a highly active new anti-HIV agent 2′,3′-didehydro-3′-deoxy-4′-ethynylthymidine. *Bioorg Med Chem Lett* **13:**3775–3777.
Johnson AA and Johnson KA (2001) Exonuclease proofreading by human mitochondrial DNA polymerase. *J Biol Chem* **276:**38097–38107.
Johnson AA, Ray AS, Hanes J, Suo Z, Colacino JM, Anderson KS, and Johnson KA (2001) Toxicity of antiviral nucleoside analogs and the human mitochondrial DNA polymerase. *J Biol Chem* **276:**40847–40857.
Johnson AA, Tsai Y, Graves SW, and Johnson KA (2000) Human mitochondrial DNA polymerase holoenzyme: reconstitution and characterization. *Biochemistry* **39:** 1702–1708.
Kasiviswanathan R, Longley MJ, Young MJ, and Copeland WC (2010) Purification and functional characterization of human mitochondrial DNA polymerase gamma harboring disease mutations. *Methods* **51:**379–384.
Kerr SG and Anderson KS (1997) RNA dependent DNA replication fidelity of HIV-1 reverse transcriptase: evidence of discrimination between DNA and RNA substrates. *Biochemistry* **36:**14056–14063.
Kim EY, Vrang L, Oberg B, and Merigan TC (2001) Anti-HIV type 1 activity of 3′-fluoro-3′-deoxythymidine for several different multidrug-resistant mutants. *AIDS Res Hum Retroviruses* **17:**401–407.
Kim J, Roberts A, Yuan H, Xiong Y, and Anderson KS (2012) Nucleocapsid protein annealing of a primer-template enhances (+)-strand DNA synthesis and fidelity by HIV-1 reverse transcriptase. *J Mol Biol* **415:**866–880.
Kirby KA, Singh K, Michailidis E, Marchand B, Kodama EN, Ashida N, Mitsuya H, Parniak MA, and Sarafianos SG (2011) The sugar ring conformation of 4′-ethynyl-2-fluoro-2′-deoxyadenosine and its recognition by the polymerase active site of HIV reverse transcriptase. *Cell Mol Biol (Noisy-le-grand)* **57:**40–46.
Koczor CA and Lewis W (2010) Nucleoside reverse transcriptase inhibitor toxicity and mitochondrial DNA. *Expert Opin Drug Metab Toxicol* **6:**1493–1504.
Kohler JJ and Lewis W (2007) A brief overview of mechanisms of mitochondrial toxicity from NRTIs. *Environ Mol Mutagen* **48:**166–172.
Kong XB, Zhu QY, Vidal PM, Watanabe KA, Polsky B, Armstrong D, Ostrander M, Lang SA Jr, Muchmore E, and Chou TC (1992) Comparisons of anti-human immunodeficiency virus activities, cellular transport, and plasma and intracellular pharmacokinetics of 3′-fluoro-3′-deoxythymidine and 3′-azido-3′-deoxythymidine. *Antimicrob Agents Chemother* **36:**808–818.
Lee H, Hanes J, and Johnson KA (2003) Toxicity of nucleoside analogues used to treat AIDS and the selectivity of the mitochondrial DNA polymerase. *Biochemistry* **42:**14711–14719.
Lee YS, Kennedy WD, and Yin YW (2009) Structural insight into processive human mitochondrial DNA synthesis and disease-related polymerase mutations. *Cell* **139:**312–324.
Lim SE, Ponamarev MV, Longley MJ, and Copeland WC (2003) Structural determinants in human DNA polymerase gamma account for mitochondrial toxicity from nucleoside analogs. *J Mol Biol* **329:**45–57.
Lin PF, Samanta H, Rose RE, Patick AK, Trimble J, Bechtold CM, Revie DR, Khan NC, Federici ME, and Li H (1994) Genotypic and phenotypic analysis of human immunodeficiency virus type 1 isolates from patients on prolonged stavudine therapy. *J Infect Dis* **170:**1157–1164.
Longley MJ, Ropp PA, Lim SE, and Copeland WC (1998) Characterization of the native and recombinant catalytic subunit of human DNA polymerase gamma: identification of residues critical for exonuclease activity and dideoxynucleotide sensitivity. *Biochemistry* **37:**10529–10539.
Michailidis E, Marchand B, Kodama EN, Singh K, Matsuoka M, Kirby KA, Ryan EM, Sawani AM, Nagy E, Ashida N, et al. (2009) Mechanism of inhibition of HIV-1 reverse transcriptase by 4′-ethynyl-2-fluoro-2′-deoxyadenosine triphosphate, a translocation-defective reverse transcriptase inhibitor. *J Biol Chem* **284:**35681–35691.
Mitsuya H, Weinhold KJ, Furman PA, St Clair MH, Lehrman SN, Gallo RC, Bolognesi D, Barry DW, and Broder S (1985) 3′-Azido-3′-deoxythymidine (BW A509U): an antiviral agent that inhibits the infectivity and cytopathic effect of human T-lymphotropic virus type III/lymphadenopathy-associated virus in vitro. *Proc Natl Acad Sci USA* **82:**7096–7100.
Murakami E, Basavapathruni A, Bradley WD, and Anderson KS (2005) Mechanism of action of a novel viral mutagenic covert nucleotide: molecular interactions with HIV-1 reverse transcriptase and host cell DNA polymerases. *Antiviral Res* **67:**10–17.
Murakami E, Feng JY, Lee H, Hanes J, Johnson KA, and Anderson KS (2003) Characterization of novel reverse transcriptase and other RNA-associated catalytic activities by human DNA polymerase gamma: importance in mitochondrial DNA replication. *J Biol Chem* **278:**36403–36409.
Nitanda T, Wang X, Kumamoto H, Haraguchi K, Tanaka H, Cheng YC, and Baba M (2005) Anti-human immunodeficiency virus type 1 activity and resistance profile of 2′,3′-didehydro-3′-deoxy-4′-ethynylthymidine in vitro. *Antimicrob Agents Chemother* **49:**3355–3360.
Paintsil E, Dutschman GE, Hu R, Grill SP, Lam W, Baba M, Tanaka H, and Cheng YC (2007) Intracellular metabolism and persistence of the anti-human immunodeficiency virus activity of 2′,3′-didehydro-3′-deoxy-4′-ethynylthymidine, a novel thymidine analog. *Antimicrob Agents Chemother* **51:**3870–3879.
Ray AS, Basavapathruni A, and Anderson KS (2002a) Mechanistic studies to understand the progressive development of resistance in human immunodeficiency virus type 1 reverse transcriptase to abacavir. *J Biol Chem* **277:**40479–40490.
Ray AS, Murakami E, Peterson CN, Shi J, Schinazi RF, and Anderson KS (2002b) Interactions of enantiomers of 2′,3′-didehydro-2′,3′-dideoxy-fluorocytidine with wild type and M184V mutant HIV-1 reverse transcriptase. *Antiviral Res* **56:**189–205.
Ray AS, Schinazi RF, Murakami E, Basavapathruni A, Shi J, Zorca SM, Chu CK, and Anderson KS (2003) Probing the mechanistic consequences of 5-fluorine substitution on cytidine nucleotide analogue incorporation by HIV-1 reverse transcriptase. *Antivir Chem Chemother* **14:**115–125.
Ray AS, Yang Z, Shi J, Hobbs A, Schinazi RF, Chu CK, and Anderson KS (2002c) Insights into the molecular mechanism of inhibition and drug resistance for HIV-1 RT with carbovir triphosphate. *Biochemistry* **41:**5150–5162.
Sohl CD, Singh K, Kasiviswanathan R, Copeland WC, Mitsuya H, Sarafianos SG, and Anderson KS (2012) Mechanism of interaction of human mitochondrial DNA polymerase γ with the novel nucleoside reverse transcriptase inhibitor 4′-ethynyl-2-fluoro-2′-deoxyadenosine indicates a low potential for host toxicity. *Antimicrob Agents Chemother* **56:**1630–1634.
Song S, Pursell ZF, Copeland WC, Longley MJ, Kunkel TA, and Mathews CK (2005) DNA precursor asymmetries in mammalian tissue mitochondria and possible contribution to mutagenesis through reduced replication fidelity. *Proc Natl Acad Sci USA* **102:**4990–4995.
Tanaka H, Haraguchi K, Kumamoto H, Baba M, and Cheng YC (2005) 4′-Ethynylstavudine (4′-Ed4T) has potent anti-HIV-1 activity with reduced toxicity and shows a unique activity profile against drug-resistant mutants. *Antivir Chem Chemother* **16:**217–221.
Vaccaro JA and Anderson KS (1998) Implication of the tRNA initiation step for human immunodeficiency virus type 1 reverse transcriptase in the mechanism of 3′-azido-3′-deoxythymidine (AZT) resistance. *Biochemistry* **37:**14189–14194.
Vaccaro JA, Parnell KM, Terezakis SA, and Anderson KS (2000) Mechanism of inhibition of the human immunodeficiency virus type 1 reverse transcriptase by d4TTP: an equivalent incorporation efficiency relative to the natural substrate dTTP. *Antimicrob Agents Chemother* **44:**217–221.
Venhoff AC, Lebrecht D, Reuss FU, Heckl-Ostreicher B, Wehr R, Walker UA, and Venhoff N (2009) Mitochondrial DNA depletion in rat liver induced by fosalvudine tidoxil, a novel nucleoside reverse transcriptase inhibitor prodrug. *Antimicrob Agents Chemother* **53:**2748–2751.
Wang L, Sun R, and Eriksson S (2011) The kinetic effects on thymidine kinase 2 by enzyme-bound dTTP may explain the mitochondrial side effects of antiviral thymidine analogs. *Antimicrob Agents Chemother* **55:**2552–2558.
Wheeler LJ and Mathews CK (2011) Nucleoside triphosphate pool asymmetry in mammalian mitochondria. *J Biol Chem* **286:**16992–16996.
Wińska P, Miazga A, Poznański J, and Kulikowski T (2010) Partial selective inhibition of HIV-1 reverse transcriptase and human DNA polymerases γ and β by thiated 3′-fluorothymidine analogue 5′-triphosphates. *Antiviral Res* **88:**176–181.
Yamanaka H, Gatanaga H, Kosalaraksa P, Matsuoka-Aizawa S, Takahashi T, Kimura S, and Oka S (2007) Novel mutation of human DNA polymerase gamma associated with mitochondrial toxicity induced by anti-HIV treatment. *J Infect Dis* **195:**1419–1425.
Yang G, Dutschman GE, Wang CJ, Tanaka H, Baba M, Anderson KS, and Cheng YC (2007) Highly selective action of triphosphate metabolite of 4′-ethynyl D4T: a novel anti-HIV compound against HIV-1 RT. *Antiviral Res* **73:**185–191.
Yang G, Paintsil E, Dutschman GE, Grill SP, Wang CJ, Wang J, Tanaka H, Hamasaki T, Baba M, and Cheng YC (2009) Impact of novel human immunodeficiency virus type 1 reverse transcriptase mutations P119S and T165A on 4′-ethynylthymidine analog resistance profile. *Antimicrob Agents Chemother* **53:** 4640–4646.
Yang G, Wang J, Cheng Y, Dutschman GE, Tanaka H, Baba M, and Cheng YC (2008) Mechanism of inhibition of human immunodeficiency virus type 1 reverse transcriptase by a stavudine analogue, 4′-ethynyl stavudine triphosphate. *Antimicrob Agents Chemother* **52:**2035–2042.

Address correspondence to: Dr. Karen S. Anderson, Department of Pharmacology, School of Medicine, Yale University, 333 Cedar Street, SHM B350, New Haven, CT 06520. E-mail: karen.anderson@yale.edu